JOURNAL OF BACTERIOLOGY, Sept. 2007, p. 6551–6563 Vol. 189, No. 18
0021-9193/07/$08.00+0 doi:10.1128/JB.00480-07

VirB1* Promotes T-Pilus Formation in the *vir*-Type IV Secretion System of *Agrobacterium tumefaciens*▽†

John Zupan, Cheryl A. Hackworth,‡ Julieta Aguilar, Doyle Ward,§ and Patricia Zambryski*

Department of Plant and Microbial Biology, Koshland Hall, University of California, Berkeley, Berkeley, California 94720-3102

Received 29 March 2007/Accepted 29 June 2007

The *vir*-type IV secretion system of *Agrobacterium* is assembled from 12 proteins encoded by the *virB* operon and *virD4*. VirB1 is one of the least-studied proteins encoded by the *virB* operon. Its N terminus is a lytic transglycosylase. The C-terminal third of the protein, VirB1*, is cleaved from VirB1 and secreted to the outside of the bacterial cell, suggesting an additional function. We show that both nopaline and octopine strains produce abundant amounts of VirB1* and perform detailed studies on nopaline VirB1*. Both domains are required for wild-type virulence. We show here that the nopaline type VirB1* is essential for the formation of the T pilus, a subassembly of the *vir*-T4SS composed of processed and cyclized VirB2 (major subunit) and VirB5 (minor subunit). A nopaline *virB1* deletion strain does not produce T pili. Complementation with full-length VirB1 or C-terminal VirB1*, but not the N-terminal lytic transglycosylase domain, restores T pili containing VirB2 and VirB5. T-pilus preparations also contain extracellular VirB1*. Protein-protein interactions between VirB1* and VirB2 and VirB5 were detected in the yeast two-hybrid assay. We propose that VirB1 is a bifunctional protein required for *vir*T4SS assembly. The N-terminal lytic transglycosylase domain provides localized lysis of the peptidoglycan cell wall to allow insertion of the T4SS. The C-terminal VirB1* promotes T-pilus assembly through protein-protein interactions with T-pilus subunits.

Bacteria have evolved a number of multiprotein complexes that mediate the translocation of macromolecules across the bacterial envelope (7, 58, 59, 67). One of these, the type IV secretion system (T4SS), directs the transport of protein(s), protein-nucleic acid complexes, or both out of the bacterial cell and into the cytoplasm of another prokaryotic or eukaryotic cell (11, 15, 52). The most common class of T4SS comprises those that mediate the conjugative transfer of plasmid DNA from donor to recipient (33, 35). The T4SS also plays essential roles in the virulence of many animal pathogens by mediating the secretion of proteinaceous effector molecules that subvert host defense mechanisms (22, 55). The best-characterized T4SS is a component of the virulence (*vir*) system of the plant pathogen *Agrobacterium tumefaciens* (13) and mediates the transfer of a nucleoprotein complex formed by the relaxase VirD2 and a single-strand DNA segment (T-strand) (reviewed in references 32, 76, and 77). In addition to the T-complex, the *vir*-T4SS also transports at least three *Agrobacterium* virulence proteins to the plant cell: VirE2, VirE3, and VirF (64, 66, 70, 71).

An understanding of the structure, as well as the operation, of the *vir*-T4SS is emerging (14, 15). This apparatus is assembled from 11 proteins encoded by the *virB* operon and an additional coupling protein, VirD4, that brings the T complex to the T4SS for export. Genetic and biochemical studies suggest that the core of the apparatus is a transmembrane complex composed of VirB6, VirB7, VirB8, VirB9, and VirB10 (10, 36, 42, 44). Energy for assembly and function of the *vir*-T4SS is provided by three ATPases—VirB4, VirB11, and VirD4 (1, 9, 17, 18, 43, 65).

The other structural feature of the *vir*-T4SS is the T pilus (31). The major component is VirB2, an F-pilin homolog (50), and VirB5 is an additional minor component (62). VirB7 also has been detected in high-molecular-weight, extracellular structures purified by centrifugation (60). Early steps in T-pilus assembly involve the intramolecular cyclization of processed VirB2 monomers (28), the formation of VirB2-VirB5 complexes in the membranes, and the formation of VirB7 homodimers (47). VirB4 interactions withVirB3 and VirB8 also facilitate T-pilus formation (74). However, exactly how VirB2 is mobilized from the inner membrane to the site of T-pilus biogenesis is not known. It has been speculated (49, 51) that chaperones and ushers, such as those that regulate the assembly of P pili (68), may deliver T-pilin subunits through the outer membrane.

VirB1, the first product of the *virB* operon, is an incompletely characterized *vir*-T4SS component. This lack of interest may stem from reports that VirB1 is not absolutely required for DNA transfer: whereas deletion of other VirB genes completely abolished DNA transfer, deletion of *virB1* reduced virulence to ≤3% (6, 8, 29). Nevertheless, these latter data suggest that VirB1 plays a significant role in *Agrobacterium*-mediated DNA transfer.

Sequence similarity between the N terminus of VirB1 and chicken egg white lysozyme and bacterial lytic transglycosylases suggests this protein provides local lysis of the peptidoglycan cell wall to create the space required for assembly of a complex as large as the T4SS (21, 45, 54). Recent data confirm this

* Corresponding author. Mailing address: Department of Plant and Microbial Biology, Koshland Hall, University of California, Berkeley, CA 94720-3102. Phone: (510) 643-9204. Fax: (510) 642-4995. E-mail: zambrysk@nature.berkeley.edu.

† Supplemental material for this article may be found at http://jb.asm.org/.

‡ Present address: Department of Biology, West Valley Community College, 14000 Fruitvale Ave., Saratoga, CA 95070.

§ Present address: Program in Molecular Medicine, University of Massachusetts Medical School, 373 Plantation St., Worcester, MA 01605.

▽ Published ahead of print on 13 July 2007.

prediction by demonstrating VirB1 transglycosylase activity in vitro (75). Interaction between VirB1 and VirB8, as well as VirB9 and VirB10, may target the lytic transglycosylase activity of VirB1 to the site of T4SS assembly (72) and suggests that VirB1 has a periplasmic function. The C-terminal third of the protein, VirB1*, is cleaved from VirB1 and secreted by an unknown mechanism (3). In *Brucella suis*, the C terminus of VirB1, although not processed, interacts with VirB9 (a periplasmic protein), which again suggests a periplasmic function for this VirB1 homolog (37). Complementation of an in-frame deletion of *virB1* with constructs expressing either the N-terminal lytic transglycosylase domain or C-terminal VirB1* resulted in tumors intermediate in size and frequency compared to the wild type (53). Thus, each domain contributes an independent function to virulence.

Here we provide genetic evidence that VirB1* is an essential factor for T-pilus assembly. A nopaline *virB1* deletion strain of *Agrobacterium* fails to mobilize VirB2 and VirB5 to the cell exterior for T-pilus biogenesis. VirB2 and VirB5 are restored to isolated T pili when the deletion is complemented with full-length VirB1 or VirB1* but not with the N-terminal lytic transglycosylase domain. Protein-protein interactions between VirB1* and both VirB2 and VirB5 were detected in the yeast two-hybrid assay. At least 50% of VirB1* is exported to the cell exterior (3), and we show that a portion of extracellular VirB1* copurifies with the T pilus. Thus, VirB1* may promote T-pilus assembly by first binding VirB2 and VirB5 and then acting as a chaperone for T-pilus subunits as they are mobilized to sites of T-pilus assembly and subsequently to the cell exterior.

MATERIALS AND METHODS

Strains and growth conditions. *A. tumefaciens* strain, C58 carrying the nopaline Ti plasmid pTiC58, served as the wild-type strain. CB1001 is a derivative of C58 with an in-frame deletion of *virB1* (62). CB1001 was complemented with the constructs described below (Table 1 and Fig. 1B).

For induction of the *vir* system, single colonies were inoculated into 5 ml of Luria broth with appropriate antibiotics and grown overnight at 28°C. The following day, cultures were diluted to an A_{600} of 0.1 in AB medium (55 mM glucose, 20 mM morpholineethanesulfonic acid, 37 mM NH_4Cl, 2 mM KCl, 1.2 mM $MgSO_4 \cdot 7H_2O$, 68 μM $CaCl_2$, 9 μM $FeSO_4 \cdot 7H_2O$, and 1 mM potassium phosphate) (49) and grown for 5 h at 20°C. For analysis of VirB1 and VirB1 variants, 3 ml of culture were centrifuged for 5 min in a table-top centrifuge, and the supernatant was removed. Cells were resuspended in approximately 0.5 ml of double-distilled H_2O and plated on 35 ml of AB medium solidified with agar (1.6%) in a 10-cm petri plate. Acetosyringone (AS) was added (200 μM final concentration) to plates to induce the *vir* system along with appropriate antibiotics. Cultures were incubated for 18 to 20 h at 19°C. For analysis of T pili, 1 ml of culture was plated on 80 ml of AB medium solidified with agar (1.6%) in a 15-cm petri plate, and subsequent analysis was performed as described previously (62).

Construction of vectors for expression of wild-type VirB1 and VirB1 mutants. All procedures for plasmid DNA isolation and manipulations, such as digestion with restriction endonucleases or ligation, were performed as described previously (61). For complementation studies, pDW029 was constructed to enhance *vir*-regulated protein expression. The ribosome-binding site (RBS) sequence and the XhoI and ClaI sites of pBP21 (53) were replaced with the RBS corresponding to *A. tumefaciens* 16S ribosomal DNA. In the introduced sequence, 5′-CTCGA *GGAGGAGGT*TTGTCATGATCGAT-3′, the RBS is in italics, and a BspHI site spanning the translation initiation codon (in boldface) is underlined. This plasmid carries the pVS1 origin of replication (40) for replication in *A. tumefaciens*. Protein expression from this promoter is ~3-fold higher relative to pBP21 as estimated by green fluorescent protein (GFP) expression (J. Zupan, D. Ward, and P. Zambryski, data not shown).

pDW101 is a pDW029 derivative that encodes full-length VirB1 from pTiC58. The *virB1* coding sequence was PCR amplified from pGK217 (48) such that a BspHI site was introduced at the initiation codon and a PstI site introduced 3′ of the termination codon. Oligonucleotides DWB1Bs165 and DWB1P_140 were used as primers for this PCR. The PCR fragment was first cloned into pCR-BluntII-Topo (Invitrogen) and then cloned as a BspHI-PstI fragment into pDW029 to create pDW101. The protein encoded by this plasmid is referred to as VirB1 throughout the text.

Amino acid substitutions and deletions in VirB1 were produced by inverse PCR (56) using pDW101 as the template. PCR products were generated with oligonucleotides described in Table 1 and then digested with appropriate restriction endonucleases, followed by ligation. Constructs were propagated in *Escherichia coli* and confirmed by sequencing.

pJZ034 encodes the VirB1 N-terminal 179 amino acids (aa), which correspond to the signal peptidase I (SPI) domain that targets the protein to the general secretory pathway (GSP) and the lytic transglycosylase domain. A stop codon was introduced after the first alanine of the VirB1* cleavage site. Oligonucleotides LysF029 and LysR029 were used as primers for inverse PCR to produce this plasmid. The protein encoded by this plasmid is referred to as VirB1-LT throughout the text.

pJZ036 encodes a protein with a large internal deletion in the VirB1 lytic transglycosylase domain. The first 10 aa after the SPI domain and the 10 aa N-terminal to the VirB1* cleavage site were retained to provide sequence context at these processing sites. Oligonucleotides B1*F029 and B1*R029 were used as primers for inverse PCR to produce this plasmid. The protein encoded by this plasmid is referred to as VirB1* throughout the text.

pJZ038 encodes VirB1 without the SPI domain. Oligonucleotides SPF029 and SPR029 were used as primers for inverse PCR to produce this plasmid. The protein encoded by this plasmid is referred to as VirB1ΔSP.

pJZ040 encodes VirB1 with two amino acid substitutions at the VirB1* cleavage site. Alanine 179 and alanine 180 were changed to proline and arginine, respectively, by the use of the nucleotide sequence for the restriction endonuclease AvrII. Oligonucleotides B1no*F029 and B1no*R029 were used as primers for inverse PCR to produce this plasmid. The protein encoded by this plasmid is referred to as VirB1(AA/PR) throughout the text.

pJZ042 encodes VirB1 with an amino acid substitution in the lytic transglycosylase active site. Glutamic acid 60 was changed to glutamine. This mutation is in a domain conserved among transglycosylases and thought to form the catalytic site (54). When this mutation has been introduced into other transglycosylases, enzymatic activity was abolished. Oligonucleotides LysE60QF029 and LysE60QR029 were used as primers for inverse PCR to produce this plasmid. The protein encoded by this plasmid is referred to as VirB1(E/Q) throughout the text.

pJZ076 is a pDW029 derivative that encodes nopaline VirB1 with a single amino acid change in the VirB1* processing site. This change, glutamine 187 to serine, produces a contiguous stretch of 19 aa that are identical to the sequence of octopine VirB1. Oligonucleotides B1QtoS.F and B1QtoS.R were used as primers for inverse PCR to produce this plasmid. The protein encoded by this plasmid is referred to as VirB1(Q/S) throughout the text.

pJZ079 is a pDW029 derivative that encodes octopine VirB1 with a hemagglutinin epitope tag at the carboxy terminus. Oligonucleotides MTX19 and OctB1HA.R2 were used as primers for PCR to introduce the coding sequence for the hemagglutinin epitope tag at the 3′ of the octopine *virB1* gene. The template for this PCR was pMTX124 (53). The PCR product was subcloned by using a topoisomerase vector (pCR-BluntII-Topo; Invitrogen). The intermediate plasmid was digested with HindIII and PstI, and the gel-purified insert was ligated into similarly digested pDW029.

pJZ093 is a pDW029 derivative that encodes octopine VirB1 with an internal hemagglutinin epitope tag between aa 188 and 189. Oligonucleotides FOctB1NcoI, 5OctB1IntHA.R, 3OctB1IntHA.F, and 3OctB1IntHA.R were used as primers for overlap extension PCR. The template was pMTX124. The PCR product was subcloned into pCR-BluntII-Topo (Invitrogen). The intermediate plasmid was digested with NcoI and PstI, and the gel-purified insert was ligated into pDW029 digested with BspHI and PstI.

Protein analysis. Preparation of the cell lysates and supernatant fractions by precipitation with acetone, as well as analysis of VirB1 products by gel electrophoresis and Western blotting, was performed as previously described (3). T-pilus isolation was performed as described earlier (38). Polyclonal anti-VirB2 antibody was generated against the peptide QSAGGGTDPATMVNN (aa 48 to 62, the N-terminal 15 aa of the mature VirB2 T pilin).

The well-documented and established procedure for isolating T pili is to remove surface structures from *vir*-induced cells by application of shearing forces such as are generated by passing a concentrated cell suspension through a small-diameter needle (2, 38, 41, 49, 50, 63). Low-speed centrifugation then separates bacterial cells from any material liberated from the cell surface by the shear forces generated in the syringe. Purification of high-molecular-weight

TABLE 1. Bacterial strains, plasmids, and oligonucleotides used in the current study

Bacterial strain, plasmid, or oligonucleotide	Relevant characteristics or sequence	Source or reference
Strains		
E. coli DH5α	F⁻ ϕ80/*lacZ*ΔM15 Δ(*lacZYA-argF*)*U169 rec endAI hsdR17*	Laboratory
A. tumefaciens		
C58	A136 containing the nopaline Ti plasmid pTiC58 stock	Laboratory
CB1001	C58 with a precise, nonpolar deletion of *virB1* from pTiC58	
Plasmids for expression in *A. tumefaciens* (protein)		
pDW029	Str^r Spc^r; BHR vector with nopaline *virB* promoter and consensus RBS	This study
pDW101 (VirB1)	pDW029 derivative; *vir*-regulated expression of full-length VirB1	This study
pJZ034 (VirB1-LT)	pDW029 derivative; *vir*-regulated expression of VirB1 lytic transglycosylase domain	This study
pJZ036 (VirB1*)	pDW029 derivative; *vir*-regulated expression of VirB1*	This study
pJZ038 (VirBΔSP)	pDW029 derivative; *vir*-regulated expression of VirB1 without SPI signal	This study
pJZ040 [VirB1(AA/PR)]	pDW029 derivative; *vir*-regulated expression of VirB1 in which the VirB18 processing site at aa 179 to 80 changed from AA to PR	This study
pJZ042 [VirB1(E/Q)]	pDW029 derivative; *vir*-regulated expression of VirB1 in which the glutamic acid (aa 60) in lytic transglycosylase catalytic site changed to glutamine	This study
pJZ71 (VirB1-B2)	pDW029 derivative; *vir*-regulated expression of wild-type VirB1 and VirB2 from wild-type, overlapping coding sequences	This study
pJZ076 [VirB1(Q/S)]	pDW029 derivative; *vir*-regulated expression of VirB1 in which glutamine (aa 182) changed to serine	This study
pJZ079	pDW029 derivative; *vir*-regulated expression of octopine VirB1 with a hemagglutinin epitope tag at the carboxy terminus	This study
pJZ093	pDW029 derivative: *vir*-regulated expression of octopine VirB1 with a hemagglutinin epitope tag inserted between aa 188 and 189	This study
Yeast two-hybrid plasmids		
pC-ACT.2.B2	Full-length VirB2 in pC-ACT.2	72
pC-ACT.2.B2m	VirB2 (aa 48 to 121) in pC-ACT.2	72
pC-ACT.2.B2(95-121)	VirB2 (aa 95 to 121) in pC-ACT.2	72
pACTII.B5ΔSP	VirB5ΔSP in pACTII	Laboratory stock
pCD.1.B1	Full-length VirB1 in pCD.1	72
pAS2.VirB1ΔSP	VirB1ΔSP in pAS2	Laboratory stock
pCD.1.B1*+44	VirB1*+44 in pCD.1	This study
pCD.1.B1*	VirB1* in pCD.1	72
Additional plasmid		
pGK217	Template for VirB1 PCR	48
Oligonucleotides		
B1*F029	5′-TCGACCTAGGTTCGCGAACGGCTACGTG-3′	
B1*R029	5′-GTTGCCTAGGAGCGCATTCGCGTGCAAA-3′	
B1no*F029	5′TAATCCTAGGCAACAGCTCGTCCCCCCGTTAACC	
B1no*F029	5′-CTCACCTAGGCGTTTCAACTTTTCGCAC-3′	
B1QtoS.F	5′-CTCGTCCCCCCGTTAACCGCG-3′	
B1QtoS.R	5′-GGATTGAGCGGCCGTTTCAAC-3′	
CH010	5′-GCGACTGCAGTTATTGCGGACCT-3′	
CH013	5′-GATGCCTAGGCTTGCTTGGGAGCCGCTA-3′	
DWB1Bs165	5′-ATCGATCATGAGCTTGGGGAGATTGGGAATG-3′	
DWB1P_140	5′-GCGACTGCAGATCGCATTATTGCGGACCTCCTTG-3′	
LysE60QF029	5′-CTCCGTCGACGCTTGCAGCGATCGCTCAGGTCCAAAGTCGCTTTGATCCGC-3′	
LysE60QR029	5′-AAGCGTCGACGGAGCAACGGATGGAGC-3′	
LysF029	5′-GTTGCCTAGGGAATTCCTGCAGCCC-3′	
LysR029	5′-TCGGCCTAGGTCAGGCCGTTTCAACTTTTCG-3′	
MTX19	5′-GGAACCTTGAGCTAAGGAGATAAGG-3′	
OctB1HA.R2	5′-GAACTGCAGCTCCTTACGCATAATCCGGGACATCATACGGGTATAAGTCGAATAAGA CTTG-3′	
FOctB1NcoI	5′-CCATGGTTAAGAGATCGGGGTCGC-3′	
5OctB1IntHA.R	5′- CGCATAATCCGGGACATCATACGGATAATCGTCTTGCGGAGGCTCGATTAA-3′	
3OctB1IntHA.F	5′-TATCCGTATGATGTCCCGGATTATGCGCACAAGGCACTAAAATCGGAAGAT	
3OctB1IntHA.R	5′-CGGAACTGCAGCACCTTAGTATAAGTCGAATAAGACTTG-3′	
SPF029	5′-AGAGTCATGATGGAGTTCAATAATTTTGCACGC-3′	
SPR029	5′-AGTAAGATAATCGACAGC-3′	
VirB1.5.BspH	5′-TTGGTCATGAGCTTGGGGAGATGGGGAATG-3′	

complexes or structures is achieved by high-speed centrifugation of the supernatant from the first centrifugation. This procedure results in the enrichment of the major and minor T-pilus subunits, VirB2 and VirB5, in the high-speed pellet from a *vir*-induced culture of wild-type *Agrobacterium*. Electron microscopy images have confirmed the purification of filamentous structures specifically from *vir*-induced cells with dimensions that correspond to T pili (62).

Isolation of periplasmic proteins was based on the procedure of De Maagd and Lugtenberg (19). Briefly, cells were harvested and resuspended in 50 mM potassium phosphate buffer (pH 5.5) and then pelleted by centrifugation at 7,000 × *g*. An aliquot of total cells was frozen in denaturing sample buffer. The remaining cells were resuspended in an osmotic shock solution of 50 mM Tris (pH 8), 20% sucrose, 2 mM EDTA, 87 μg of phenylmethylsulfonyl fluoride/ml, and 200 μg of lysozyme/ml, followed by incubation at room temperature for 30 min. The mixture was centrifuged at 7,000 × *g*, and the supernatant (periplasmic fraction) was concentrated by acetone precipitation.

Sequence comparisons. To determine whether other bacterial species showed conservation of the VirB1* domain, we first performed a PSI-BLAST search with *A. tumefaciens* (strain C58) VirB1 (NP_536285.1) residues 168 to 252 against the nonredundant database. In the second iteration of the search, 12 sequences were identified with an E-value of 0.005 or better, including a probable VirB1 protein from *M. loti* (CAD31462). No new sequences were found in subsequent iterations.

To search more broadly for homologs, we aligned *A. tumefaciens* (C58) VirB1, the *M. loti* probable VirB1, and the *B. abortus* VirB1 (AAF73894) by using

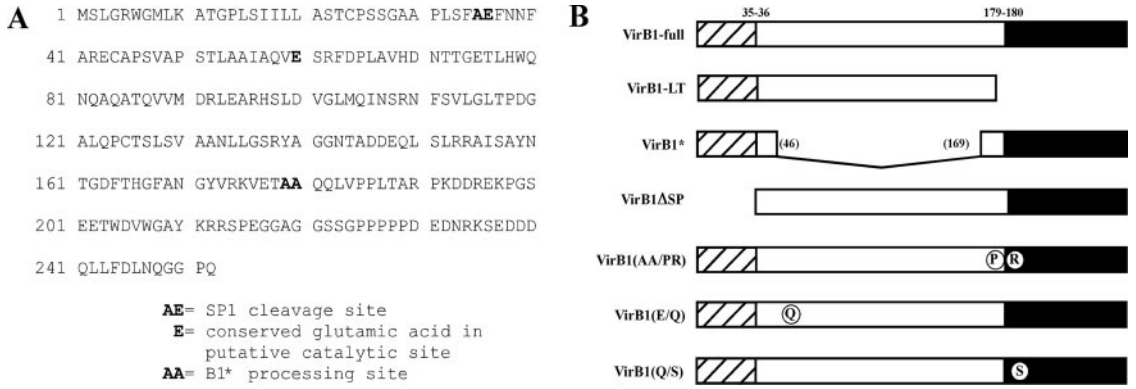

FIG. 1. VirB1 amino acid sequence and diagrams of wild-type VirB1 and VirB1 deletion and mutant derivatives. (A) Amino acid sequence of nopaline VirB1 (NCBI, NP_536285.1). Critical amino acids in the SPI processing site, lytic transglycosylase active site, and VirB1* processing site are in boldface. (B) Diagrams of wild-type VirB1, VirB1 deletion mutants, and VirB1 mutants with amino acid changes expressed from complementation plasmid pDW029 in CB1001, a *virB1* deletion strain of C58. The hatched area indicates the signal peptide for the GSP. The white area is the region of lytic transglycosylase similarity. The black area indicates VirB1*. Numbers indicate amino acid positions.

MUSCLE (27). The alignment was cropped to exclude all but the C-terminal domain of VirB1, from aa 154 to the end, using the alignment editor Jalview (16). A hidden Markov model (HMM) was constructed by using the program Hmmbuild on the cropped alignment (26). Sequences matching the HMM were selected from the Uniprot database by using the Hmmsearch program and aligned to the model by using the Hmmalign program. The new alignment was cropped to the relevant region, edited to remove redundancy, and then used as the basis for building another HMM. The process was repeated, resulting in a final multiple sequence alignment of 27 homologs.

Yeast two-hybrid analysis. Protein-protein interactions were characterized by the yeast two-hybrid system (25). Coding sequences for full-length fragments of VirB1 were cloned in fusion to the Gal-4 DNA-binding domain in either the *CEN* vector, pCD.2 (72), or the 2μm vector, pAS2 (24). Coding sequences for full-length protein or fragments of VirB2 were cloned in fusion to the Gal-4 activation domain in the *CEN* vector, pC-ACT.2 (25, 72) or the 2μm vector, pACTII (24). To construct pCD.B1*+44, the nucleotide sequence encoding VirB1* and the 44 aa N-terminal to the VirB1* cleavage site was PCR amplified from pAS2.B1ΔSP with oligonucleotides CH010 and CH013 (Table 1). The restriction site for AvrII was introduced at the 5′ end of the coding sequence and PstI at the 3′ end of the PCR product. The PCR product was purified, digested with AvrII and PstI, and ligated into similarly restricted pCD.1 to produce pCH001. In addition, laboratory stock plasmids pAS2.B1ΔSP and pACTII.B5ΔSP were constructed as described previously (4). Briefly, the coding sequence for VirB1ΔSP and VirB5ΔSP were PCR amplified, digested with appropriate restriction endonucleases, and ligated to pACTII (24). Yeast two-hybrid plasmids were transformed into yeast strain YD116 (25), and interactions were detected by growing transformants on appropriate selective media (25). Interactions were quantified by β-galactosidase activity using chorophenol-red-β-D-galactopyranoside substrate (CPRG; Roche Chemical) as described previously (24).

Transmission electron microscopy. Bacterial cells were adjusted to an A_{600} of 2.0 in 50 mM potassium phosphate buffer (pH 7) and deposited on carbon-Formvar films on 200 mesh, 3-mm copper grids. Then, 10 μl of bacterial suspension was placed on each grid for 2 to 3 min to allow bacteria to settle on the grid. Excess cell suspension was then wicked away, and each grid was washed three times by floating it on a drop of water for a few seconds. Grids were then stained with 1% phosphotungstic acid–0.01% glucose (pH 7) for 1 min. The specimens were examined in a FEI Tecnai 12 transmission electron microscope.

A. tumefaciens C58 cells were grown, and *vir* gene expression was induced with 200 μM AS. After 24 h of induction the bacterial cells were transferred to copper disks (50 μm thick, 1.44 mm in diameter) and frozen by using a Bal-Tec HPM 010 high-pressure freezer. Frozen samples were maintained under liquid nitrogen and transferred into a 2-ml cryovial containing 0.2% glutaraldehyde and 0.1% uranyl acetate in anhydrous acetone. The samples were placed into the Bal-Tec HPM 010 unit, freeze substituted under controlled temperatures, and then brought up to 0°C over 72 h. Samples were covered in LR white resin and polymerized in a microwave at 650 W for 45 min. Embedded samples were sectioned with the Ultramicrotome-MT 6000. Ultrathin sections (60 nm) were collected on Formvar 100 mesh nickel grids coated and treated by ion discharge in a vacuum evaporator.

For immunogold labeling, grids containing bacterial sections were sequentially placed on a 20-μl drop of the following solutions: (i) 0.1% glycine for 15 min to quench unreacted aldehyde groups; (ii) 5% normal goat serum (blocking agent) for 15 min; (iii) primary antibody (α-VirB1) diluted 1:500 in blocking agent at 4°C overnight; (iv) three washes in 0.5 M NaCl in phosphate-buffered saline (PBS) of 5 min each; (v) five washes in PBS–0.2%Tween for 3 min each; (vi) five washes in PBS for 3 min each; (vii) secondary antibody buffer (1% bovine serum albumin, 0.1% cold water fish gelatin, 0.25% Tween 20) for 15 min; (viii) secondary antibody (10-nm gold conjugated goat anti-rabbit) diluted 1:200 in secondary antibody buffer for 60 min at room temperature; (ix) five washes in PBS–0.2% Tween for 5 min each; (x) five washes in PBS for 3 min each; (xi) 0.5% glutaraldehyde in PBS for 10 min; (xii) one wash in PBS for 1 min; and (xiii) five washes in water for 1 min each. The grids were then stained with 2% uranyl acetate and lead citrate. Samples were observed and photographed by using an FEI Tecnai 12 100 kV transmission electron microscope.

Tumor studies. Tumor assays on *Kalachoe diagremontiana* were performed as previously described (53). Briefly, 1-cm wound sites were created by carefully scratching the surface of a leaf with a razor blade. Wounds were immediately inoculated with 10^9 CFU (resuspended in 10 μl of double-distilled H_2O) of the strains described. We determined that this concentration of bacteria is optimal for reproducibly inciting tumors by testing different dilutions of bacteria. Each strain was inoculated multiple times on several independent plants. Inoculated plants were incubated at 19°C for 48 h and then transferred to room temperature. The fraction of inoculations that incited the tumors was calculated. The sizes of the tumors relative to that of tumors incited by A348 (wild type) were estimated by visual inspection on a scale of 0 to 4. The mean relative tumor size incited by each strain was then calculated. Relative tumorigenesis was quantified as follows: (tumor frequency × tumor size × 0.25) × 100; a strain that produces tumors of maximal size in every inoculation would then have a relative index of 100%.

RESULTS

A. tumefaciens strains with an in-frame deletion of *virB1* do not produce T pili containing VirB2 and VirB5 (30, 49, 62). We assayed the ability of the full-length *virB1* and *virB1* mutants to restore wild-type T-pilus formation in a *virB1* deletion strain to determine whether the N-terminal lytic transglycosylase domain or C-terminal VirB1* contribute to T-pilus formation. The role of VirB1 in T-pilus formation was further characterized by the identification of protein-protein interactions between VirB1* and T-pilus subunits, VirB2 and VirB5.

Expression of VirB1 and derivatives. Figure 1A shows the amino acid sequence of wild-type nopaline VirB1 (NP_536285.1) (34). Residues flanking the SPI cleavage site, the glutamic acid

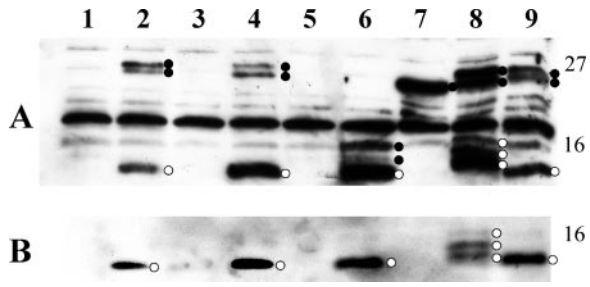

FIG. 2. Expression, C-terminal processing, and secretion of C-terminal processing products of wild-type VirB1 and VirB1 derivatives. (A) Western blot of cell pellets probed with anti-VirB1 antibody showing protein expression by *virB1* constructs. Initial translation products for each construct before and after removal of SPI domain are indicated by closed circles to the right of each lane. Products processed from the C terminus of VirB1 are indicated by open circles to the right of each lane. (B) Western blot of precipitated supernatant showing secreted VirB1* or other C-terminal products from VirB1 indicated by open circles to the right of each lane. Numbers to the right of each panel indicate molecular mass standards in kilodaltons. For both panels: C58 –AS (lane 1), C58 +AS (lane 2), CB1001 +AS (lane 3), CB1001 (VirB1) +AS (lane 4), CB1001(VirB1-LT) +AS (lane 5), CB1001(VirB1*) +AS (lane 6), CB1001(VirB1ΔSP) +AS (lane 7), CB1001(VirB1[AA/PR]) +AS (lane 8), CB1001(VirB1[E/Q]) +AS (lane 9). AS is an inducer of *vir* expression. −, Culture not induced by AS; +, culture induced by AS.

presumed to be required for catalytic activity of the N terminus (54), and residues flanking the C-terminal processing site for VirB1* (3) are highlighted. Figure 1B diagrams the domains of wild-type VirB1 and six deletion or mutant derivatives used in our complementation studies. VirB1-LT comprises the N terminus, including the SPI domain. VirB1* includes the N-terminal SPI domain and the C-terminal VirB1* (10 wild-type amino acids adjacent to each of these domains are also encoded for sequence context at the two cleavage sites). VirB1ΔSP contains all of VirB1 except the N-terminal 35 aa. VirB1(AA/PR) is full-length VirB1 in which the alanine-alanine VirB1* processing site is changed to proline-arginine. VirB1(E/Q) is full-length VirB1 in which the glutamic acid (aa 60) required in the active site is changed to glutamine. VirB1(Q/S) is full-length VirB1 in which a glutamine (aa 182) near the VirB1* processing site is changed to serine. This change makes the processing site region identical to that found in octopine VirB1 (see Fig. 6, below).

Note, the complementing constructs utilized here are distinct from similar constructs used in our previous study (53) since they are cloned into a different vector, pDW029 (see Materials and Methods), which yields higher expression levels. Two of the complementing constructs, VirB1 and VirB1ΔSP, employ coding sequences identical to those used in our previous study (53). Two constructs, VirB1-LT and VirB1*, differ slightly due to different cloning strategies. Three of the complementing constructs are new, VirB1(AA/PR), VirB1(E/Q), and VirB1(Q/S).

To assess expression and C-terminal processing of VirB1 and VirB1 mutants, whole cells from the wild-type strain C58, the *virB1* deletion strain CB1001 (62), and CB1001 complemented with the constructs described in Fig. 1B were subjected to Western blot analysis (Fig. 2A). To assess secreted forms of VirB1, cell surface proteins were released from the cell surface by vortexing and then precipitated and subjected to Western blot analysis (Fig. 2B).

In cells, full-length wild-type VirB1 is observed as a doublet migrating at approximately 26 kDa (Fig. 2A, lanes 2 and 4). The larger protein is the initial translation product. The slightly smaller protein likely results from translocation to the periplasm via the GSP, which removes the N-terminal SPI domain (35 aa in VirB1). In support of this, VirB1ΔSP was observed only as a single protein (Fig. 2A, lane 7), corresponding to the lower protein band seen in lanes 2 and 4 (and lanes 8 and 9, see below). VirB1-LT was not detected (Fig. 2A, lane 5) because our anti-VirB1 antibody does not recognize the N terminus. However, an increase in tumor formation by a *virB1* deletion strain containing VirB1-LT suggests that this deletion product is expressed and functional (see Table 2) (53). The VirB1* construct also yielded two novel proteins that are approximately the correct size for the full-length VirB1* protein that would be produced before and after cleavage of the SPI domain (Fig. 2A, lane 6). The mutations with amino acid changes at the VirB1* processing site and the catalytic site in the lytic transglycosylase domain produce abundant amounts of the full-length proteins, again as doublets (Fig. 2A, lanes 8 and 9).

Little is known about the processing of VirB1* from VirB1. VirB1* contains the C-terminal 73 aa of VirB1, is detected within an hour of VirB1 expression, and migrates anomalously at approximately 12 kDa (3). Full-length VirB1 expressed in *trans* in the *virB1* deletion strain produced more VirB1* than wild-type C58 (Fig. 2A, lanes 2 and 4). The slight overproduction may reflect that *vir*-induced expression from the pDW029 vector plasmid was enhanced by placing the start codon in close proximity to the RBS. The strain expressing only VirB1* also produced abundant amounts of VirB1* (Fig. 2A, lane 6). VirB1* was not produced when the SPI domain was deleted (Fig. 2A, lane 7). Thus, processing of VirB1* from VirB1 is mediated by a periplasmic protease or is an autocatalytic process that requires the periplasmic environment.

Unexpectedly, three C-terminal products, slightly larger than bona fide VirB1*, were produced by the strain that expressed VirB1(AA/PR), mutated at the VirB1* processing site (Fig. 2A, lane 8). The same proteolytic mechanism that produces wild-type VirB1* may also cleave at secondary sites that are not utilized when the wild-type sequence is available. Alternatively, substitution of PR for AA may render the mutant protein susceptible to

TABLE 2. Effect of *virB1* deletion on virulence of *A. tumefaciens* on *K. diagremontiana* and complementation with *virB1* and *virB1* mutants

Strain (VirB1 variant)	Tumor frequency[a]	Mean relative tumor size[b]	Relative tumor index (%)[c]
A348	0.9 (40)	4	90
A348ΔB1	0.16 (40)	0.5	1.8
A348ΔB1 (VirB1)	1.0 (16)	4	100
A348ΔB1 (VirB1-LT)	0.56 (16)	2	28
A348ΔB1 (VirB1*)	0.56 (16)	2	28
A348ΔB1 (VirB1ΔSP)	0.25 (16)	1	6.25
A348ΔB1 [VirB1(AA/PR)]	0.56 (16)	2	28
A348ΔB1 [VirB1(E/Q)]	0.43 (16)	2	22

[a] Fraction of inoculations that incited tumors (number of inoculations).
[b] Size of tumors relative to that of tumors incited by A348 (wild type) estimated by visual inspection on a scale of 0 to 4.
[c] Calculated as: [(tumor frequency × relative tumor size)/4] × 100.

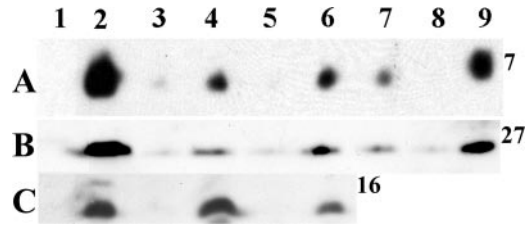

FIG. 3. Complementation of T-pilus formation in CB1001. (A) Western blot of isolated T-pili probed with anti-B2 antibody. (B) Western blot of isolated T pili probed with anti-B5 antibody. (C) Western blot of isolated T pili probed with anti-VirB1 antibody. For all panels: C58 –AS (lane 1), C58 +AS (lane 2), CB1001 +AS (lane 3), CB1001(VirB1) +AS (lane 4), CB1001(VirB1-LT) +AS (lane 5), CB1001(VirB1*) +AS (lane 6), CB1001(VirB1ΔSP) +AS (lane 7), CB1001(VirB1[AA/PR]) +AS (lane 8), CB1001(VirB1[E/Q]) +AS (lane 9). Numbers to the right of each panel indicate molecular weight standards in kDa. AS is an inducer of *vir* expression. –, Culture not induced by AS; +, culture induced by AS.

another periplasmic protease(s) that cleaves at a different site(s). Mutation of glutamic acid to glutamine in the active site of the lytic transglycosylase domain did not affect processing of VirB1* from VirB1 (Fig. 2A, lane 9).

We next assayed for VirB1* secretion to the exterior of the bacterial cells versus that present in whole cells described above. In assays for secreted VirB1* and isolated T pili (below), control Western blots were probed with anti-VirB8 antiserum to determine whether these fractions contained whole cells. VirB8 was not detected even after prolonged exposure of films, suggesting that these fractions were not contaminated with whole cells (data not shown).

Slightly more VirB1* is secreted by CB1001 expressing wild-type VirB1 in *trans* compared to C58 (Fig. 2B, lanes 2 and 4) (likely due to enhanced expression mentioned above), although the amounts secreted are approximately proportional to the amounts in whole-cell pellets. CB1001 expressing VirB1* also efficiently secreted this protein (Fig. 2B, lane 6). Since CB1001 expressing VirB1ΔSP did not produce VirB1* (Fig. 2A, lane 7), no VirB1* was secreted (Fig. 2B, lane 7). Of the three products derived from the C terminus of VirB1(AA/PR) in CB1001 expressing VirB1(AA/PR), the two lower-molecular-weight forms are secreted to a higher level than the largest-molecular-weight form (Fig. 2B, lane 8), reflecting their higher production in whole cells. CB1001 expressing VirB1(E/Q) secreted VirB1* (Fig. 2B, lane 9). Thus, the lytic transglycosylase function of the N terminus of VirB1 is not required for secretion of VirB1*.

As in our previous study (53), deletion of *virB1* reduced tumorigenesis by 90 to 99% and expression of full-length VirB1 restored wild-type virulence (Table 2). The two strains that express VirB1 with an intact lytic transglycosylase domain but that carry a deletion or mutation of the VirB1* domain [VirB1-LT and VirB1(AA/PR)] were restored to 28% of wild-type virulence. Similarly, the two strains that express VirB1 with a large deletion or mutation in the lytic transglycosylase domain [VirB1* and VirB1(E/Q)] were restored to 28 and 22% of wild-type virulence, respectively. Expression of VirB1ΔSP in the *virB1* deletion restored virulence to ca. 6% of the wild type. This latter result is an increase in virulence over the previous study (53) and may be related to the enhanced expression from the plasmid used for complementation experiments in the present study (see also the discussion of T-pilus formation in this strain below).

Analyses of VirB2 and VirB5 in isolated T pili. We next used established procedures for purification of T pili (2, 38, 41, 49, 50, 63) whereby T pili are first sheared from the surface of *vir*-induced cells and then concentrated by high-speed centrifugation. Although VirB2 is abundant in T-pilus preparations from the wild-type strain, VirB2 is not detected in the same fraction from the *virB1* deletion strain CB1001 (Fig. 3A, lanes 2 and 3). *trans* complementation of CB1001 with a plasmid that expresses full-length VirB1 restores VirB2 to the high-speed pellet but not to wild-type levels (Fig. 3A, lanes 2 and 4). VirB2 is also recovered in the T-pilus preparation specifically from CB1001 expressing VirB1* or VirB1(E/Q), the lytic transglycosylase active-site mutation (Fig. 3A, lanes 6 and 9). CB1001 complemented with VirB1* or full-length VirB1 produce comparable amounts of extracellular VirB2 (Fig. 3A, lanes 4 and 6).

There are two unexpected and interesting results from the study of isolated T pili in different complementing strains. First, VirB2 is more abundant in the high-speed pellet of CB1001 complemented with VirB1(E/Q) (Fig. 3A, lane 9) than complemented with wild-type VirB1 (Fig. 3A, lane 4). Potentially in the absence of lytic transglycosylase activity, the periplasm may be less accessible to proteases, and VirB2 T-pilus subunits may be more stable. Second, *trans* complementation with VirB1ΔSP resulted in the accumulation of a small but detectable and reproducible amount of VirB2 in the T-pilus preparations (Fig. 3A, lane 7). Since this VirB1 variant more efficiently binds the mature form of VirB2 than VirB1* (shown below in Table 3), we suggest that its binding to VirB2 mediates a small amount of VirB1ΔSP transport to the periplasm. Such periplasmic VirB1ΔSP then may be processed to produce a minute amount of VirB1* (not detected by Western blotting, Fig. 2A, lane 7, and Fig. 2B, lane 7) to facilitate VirB2 transit to the cell exterior for T-pilus generation. The partial function of VirB1ΔSP is supported by tumor assays (Table 2).

trans complementation with VirB1-LT does not restore accu-

TABLE 3. Yeast two-hybrid interactions between VirB1 constructs and VirB2 and VirB5 constructs

DNA-binding domain plasmid	Mean Miller units (SD) for activation domain plasmid[a]:				
	pC-ACT.2.B2 (aa 1–121)	pC-ACT.2.B2m (aa 48–121)	pC-ACT.2.B2 (aa 95–121)	pC-ACT.2.B5 (aa 24–220)	pC-ACT.2
pCD.1.B1	6 (0.5)	6 (0.8)	8 (0.4)	22 (0.9)	0.02 (0.03)
pAS2.B1ΔSP	29 (1.3)	292 (3)	9 (0.3)	7 (0.2)	ND
pCD.1.B1*+44	80 (4.0)	124 (9)	3 (0.2)	155 (9)	−0.01 (0.02)
pCD.1.VirB1*	11 (1.2)	44 (2)	3 (0.2)	132 (3)	ND

[a] $n = 3$. ND, no data because of poor growth.

mulation of VirB2 in T-pilus preparations (Fig. 3A, lane 5). VirB2 is also not found in the T-pilus preparation when CB1001 is *trans* complemented with VirB1(AA/PR), the VirB1* processing site mutant (Fig. 3A, lane 8). Although CB1001 expressing VirB1(AA/PR) processes and secretes products from the C terminus of VirB1 (Fig. 2B, lane 8), these fragments do not mediate accumulation of VirB2 in T-pilus preparations. These data suggest that sequences at the N terminus of VirB1* are critical for function. Variation in the amount VirB2 in cell lysates of these strains was minor (data not shown), and the data shown are representative of several independent experiments. Thus, experimental variation is not a contributing factor to the abundance of T pili. It is not known whether the reduction in VirB2 and VirB5 in preparations of T pili reflect fewer T pili per cell or shorter T pili. In summary, restoration of VirB2 to T-pilus preparations from the *virB1* deletion strain is maximal when the *trans* complementing plasmid expresses bona fide VirB1* that is secreted to the cell exterior.

VirB5 accumulation in T-pilus preparations mirrors that found for VirB2. Complementation of CB1001 with wild-type VirB1 resulted in the reappearance of VirB5 in T-pilus preparations (Fig. 3B, lanes 3 and 4). Expression of VirB1* was as effective as full-length VirB1 in restoring accumulation of VirB5 in isolated T pili (Fig. 3B, lanes 4 and 6). As for VirB2, accumulation of VirB5 was slightly higher in T pili from CB1001 expressing VirB1(E/Q) compared to full-length VirB1 (Fig. 3B, lanes 4 and 9).

These data highlight that the stoichiometry between VirB2 and VirB5 is consistent in all T-pilus preparations (Fig. 3A and B, lanes 2, 4, 6, 7, and 9). As shown above with VirB2, accumulation of VirB5 was partially supported by *trans* complementation with VirB1ΔSP (Fig. 3B, lane 7). *trans* complementation with VirB1-LT or VirB1(AA/PR) (Fig. 3B, lanes 5 and 8), however, did not increase the accumulation of VirB5 in T pili relative to CB1001. Therefore, both the major and minor T-pilus components, VirB2 and VirB5, are significantly reduced in the high-speed pellet from a *virB1* deletion strain, and their presence is restored by *trans* complementing plasmids that express and secrete VirB1*. In contrast, the lytic transglycosylase domain of VirB1 does not contribute to the accumulation of VirB2 and VirB5 in isolated T pili. Reduced levels of VirB2 and VirB5 in CB1001 extracts are not due to decreased transcription, since both proteins are found in cell pellets in amounts comparable to wild type (data not shown). Potentially, translational coupling plays a role in VirB1 mediated processing of VirB2 for pilus biogenesis.

Notably, VirB1* copurifies with T pili in wild-type cells and not in CB1001 (Fig. 3C, lanes 2 and 3). This association is found in all strains that produce VirB1* (Fig. 3C, lanes 2, 4, and 6) but not in strains only producing the N terminus of VirB1 (Fig. 3C, lane 5). We do not intend to imply that VirB1* is a structural component of T pili; indeed, VirB1* can be removed from *vir*-induced T-pilus-containing cells by vortexing. Nevertheless, that VirB1* is found in isolated T pili provides supportive evidence for a role for VirB1* in T-pilus formation.

Visual detection of T pili. In C58 grown under virulence gene-inducing conditions, the T pilus was identified as a filamentous structure that is shorter than a flagellum with a much smaller diameter (Fig. 4A) (30, 49). This structure was present

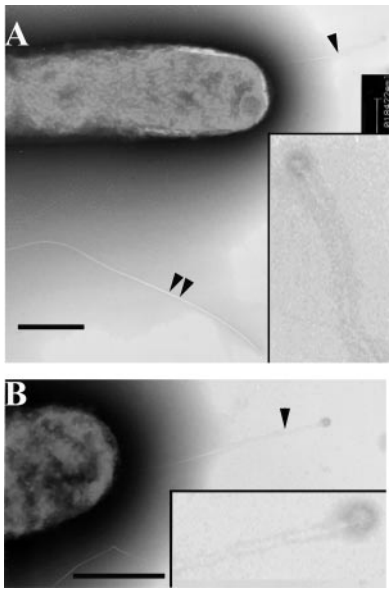

FIG. 4. Transmission electron microscopy analysis of T-pilus production by C58 and CB1001. (A) C58 +AS; (B) CB1001(VirB1) +AS. Insets in panels A and B show T pili with knob-like distal ends. T pili are indicated by single arrowheads. Flagella are indicated by a double arrowhead. AS is an inducer of *vir* expression. +AS, culture induced by AS. Scale bar, 500 nm.

in ca. 50% of the cells observed ($n > 100$). This number is lower than 100% since T pili are notoriously sensitive to loss during sample preparation for transmission electron microscopy. T pili were often inserted close to the cell pole. T pili were never observed in uninduced cells (data not shown). Vegetative flagella were less frequent under virulence gene-inducing conditions as previously reported (49). T pili were never observed on the *virB1* deletion strain CB1001 (data not shown). When CB1001 was complemented with *virB1*, T-pilus biogenesis was restored (Fig. 4B). In some cases, the tip of the T pilus contained a knob-like structure (insets in Fig. 4A and 4B). Similar structures were reported in isolated T pili (2), although whether these structures were at the base or distal tip of the isolated T pili could not be determined. The present data suggest the knob occurs at the distal tip of the T pili.

Subcellular localization of VirB1*. Previous studies have found VirB1* in the membrane (69) and soluble (62) fractions, as well as in the medium of *vir*-induced cultures (3). Here we specifically assayed for whether VirB1* fractionates with the periplasm. Periplasmic extracts were prepared from uninduced and *vir*-induced cultures and their Vir protein composition was assayed by Western blotting. Several controls for the purity of the fractionation were performed. First, inner membrane-localized VirB8 was not detected in the periplasmic fraction (Fig. 5B, lane 6). Second, VirB9 has been demonstrated to fractionate with membranes, as well as the periplasm (23); indeed, VirB9 was abundant in our periplasm fraction (Fig. 5C, lane 6). Thus, the periplasmic fraction was uncontaminated by membranes or intact cells. VirB1*, but not full-length VirB1, was detected in the periplasmic fraction (Fig. 5A, lane 6). Localization of VirB1* in the periplasm of *vir*-induced cells was confirmed by immunogold labeling (Fig. 5D). VirB1* periplas-

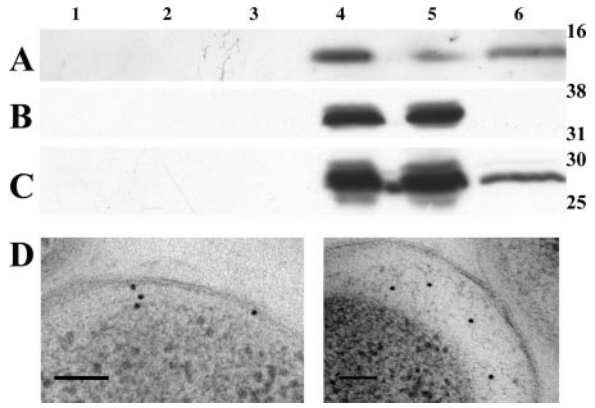

FIG. 5. Subcellular localization of VirB1*. Periplasmic fractions prepared from uninduced (lanes 1 to 3) and *vir*-induced (lanes 4 to 6) cultures of C58. (A) Western blot probed with anti-VirB1 antibody. (B) Western blot probed with anti-VirB8 antibody. (C) Western blot probed with anti-virB9 antibody. Lanes: 1 and 4, whole-cell lysate; 2 and 5, cell pellet after osmotic shock; 3 and 6, periplasm. Numbers to the right of each panel indicate molecular mass standards in kilodaltons. (D) Transmission electron micrograph of cell from an induced culture. Gold particles (10 nm) indicate localization of VirB1* in the periplasm.

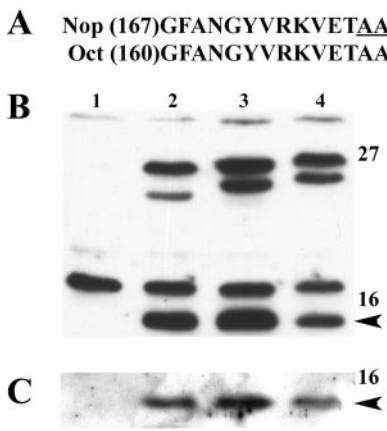

FIG. 6. Processing and secretion of nopaline VirB1(Q/S). (A) Amino acid sequences surrounding the VirB1* processing site for nopaline (Nop) and octopine (Oct) VirB1. The pair of alanines that constitute the VirB1* processing site in nopaline VirB1 are underlined. A single amino acid (*) in this region differs between nopaline and octopine. Numbers indicate the amino acid position. (B) Western blot of cell pellets probed with anti-nopaline VirB1 antibody. (C) Western blot of precipitated supernatant showing secreted VirB1*. For panels B and C: C58 –AS (lane 1), C58 +AS (lane 2), CB1001 (VirB1[Q/S]) +AS (lane 3), A348ΔB1 (VirB1[Q/S] +AS (lane 4). It is interesting that VirB1 (Q to S) without the signal peptide migrates slower than the wild-type nopaline VirB1 (without its signal peptide). However, once VirB1* is processed and cleaved from this precursor, both VirB1* derivatives that contain either Q or S very close to their N termini now migrate identically. Possibly, the Q-to-S mutation affects protein conformation, causing it to run anomalously. There also appears to be a difference between the nopaline and octopine strains in the migration of VirB1 (Q to S). Numbers to the right of each panel indicate molecular mass standards in kilodaltons. Arrowheads indicate VirB1*. AS is an inducer of *vir* expression. –, Culture not induced by AS; +, culture induced by AS.

mic localization is consistent with a role of VirB1* in interacting with VirB2 and VirB5 during T-pilus formation.

Homologs of nopaline VirB1*. Except for nopaline VirB1*, the processing and secretion of a C-terminal fragment from VirB1-like proteins has not been reported. To begin to assess whether this posttranslational modification occurs in other systems, we examined VirB1 from the octopine strain of *A. tumefaciens*. In a contiguous stretch of 19 aa that contains the nopaline VirB1* processing site, the nopaline and octopine strains differ at a single residue, glutamine (aa 182) in the nopaline strain and serine (aa 175) in the octopine strain (Fig. 6A). This amino acid difference was introduced into the nopaline VirB1 to produce VirB1 (Q/S), which was expressed in *virB1* deletions in both the nopaline strain (CB1001) and the octopine strain (A348ΔB1). VirB1* was processed (Fig. 6B) and secreted (Fig. 6C) from VirB1 (Q/S) in both the nopaline (lane 3) and the octopine (lane 4) strains, These data suggest that both strains are able to process and secrete VirB1* from a VirB1 variant whose amino acid sequence around the processing site is identical to octopine VirB1 (pTiA6).

Although A348 appears to have the capacity to process and secrete a nopaline/octopine hybrid VirB1*, octopine VirB1* has not been reported. Figure 7B shows that a protein of approximately the expected 13 kDa was detected with an anti-hemagglutinin antibody in *vir*-induced cell lysates of A348ΔB1 that expressed wild-type octopine VirB1 with hemagglutinin epitope tags (Fig. 7B, lanes 2 and 4). Epitope tags (Fig. 7A) were placed at the C terminus of octopine VirB1 (pJZ079) or between aa 188 and 189 (pJZ093), 12 aa downstream from the conserved region close to the processing site, see below). Octopine VirB1* with the internal hemagglutinin tag was efficiently processed from octopine VirB1 (Fig. 7, lane 4). VirB1* with the C-terminal hemagglutinin tag was also processed from VirB1 but at much lower efficiency (Fig. 7, lane 2). Thus, octopine VirB1 is also processed to release octopine VirB1*.

Next, we searched the databases for transglycosylases that also contain distal sequences with homology to the C-terminal VirB1* processing site. Twenty-seven homologs were detected, and the conservation around the VirB1* processing site is illustrated in Fig. 8. Interestingly, the sequences distal to the processing site are highly diverged (see Fig. S1 in the supplemental material), suggesting that these protein domains may have evolved according to the requirements of their respective biological systems. Nevertheless, the significant conservation around the VirB1* processing site suggests that C-terminal protein processing may be more common than heretofore assumed.

VirB1 protein-protein interactions. The role of VirB1* in T-pilus synthesis was addressed further by determining whether VirB1* interacts directly with T-pilus components. To this end, VirB1 and three deletion derivatives were cloned into yeast two-hybrid vectors. In one construct, the coding sequence for the SPI domain was deleted. The other two deletion constructs expressed either VirB1* or VirB1* plus the 44 aa N-terminal to VirB1* (referred to as VirB1*+44). Before embarking on two-hybrid studies, we tested for the efficiency of yeast transformation with our different plasmid constructs. Surprisingly, transformation of yeast with plasmids carrying *virB1ΔSP* and *virB1** was 2 orders of magnitude less efficient than transformations with full-length *virB1* or *virB1*+44* (Fig.

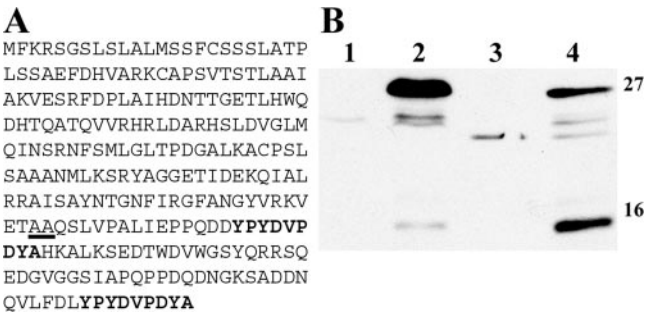

FIG. 7. Processing of hemagglutinin-tagged octopine VirB1 by an octopine strain of *A. tumefaciens.* (A) Amino acid sequence of octopine VirB1 (pTiA6). The putative VirB1* processing site is underlined, and the internal (pJZ093) and C-terminal (pJZ079) hemagglutinin sequences are indicated in boldface. (B) Western blot of whole-cell extracts probed with anti-hemagglutinin antibody. Lanes 1 and 2 contain whole-cell extracts of the octopine *virB1* deletion strain A348ΔB1 carrying pDW029 with *vir*-inducible octopine VirB1 with a C-terminal hemagglutinin tag. Lanes 3 and 4 contain whole-cell extracts of the octopine *virB1* deletion strain A348ΔB1 carrying pDW029 with *vir*-inducible octopine VirB1 with a hemagglutinin tag between aa 188 and 189 (16 aa from the putative octopine VirB1* processing site). Lanes 1 and 3 were from uninduced cultures. Lanes 2 and 4 were from cultures induced with AS. Numbers to the right of each panel indicate molecular mass standards in kilodaltons.

9A). Our interpretation is that VirB1ΔSP and VirB1* adopt conformations that expose a domain in the C terminus that is toxic to yeast. The conformations of full-length VirB1 and VirB1*+44 presumably mask the toxic domain. Interestingly, VirB1* toxicity is also alleviated by coexpression of the mature but uncyclized form of VirB2 (Fig. 9B); these data suggest that protein-protein interaction may mask the toxic domain.

These data prompted us to evaluate VirB1 interactions with T-pilus components by using the two-hybrid assay (Table 3). The strongest interactions between VirB1 (or its variants) and VirB2 (or its variants) were obtained with VirB1ΔSP or VirB1*+44 and VirB2m, which corresponds to the mature T-pilus subunit prior to cyclization. A moderately strong interaction was obtained with VirB1*+44 and full-lengthVirB2. VirB1* interacted moderately with VirB2m. Strong interactions were also detected between VirB1*+44 or VirB1* and VirB5ΔSP. In summary, interaction between VirB1* and VirB2 or VirB5 is consistently detected. The VirB2 interaction domain appears to reside in the N terminus of the mature T-pilin subunit (aa 48 to 94), since the C-terminal VirB2 (aa 95 to 121) interacts extremely poorly with VirB1 derivatives. The VirB5 interaction domain was not more narrowly defined.

These data provide independent data to suggest VirB1* interacts with VirB2 and VirB5. Protein-protein interactions are consistent with a role of VirB1* in facilitating T-pilus formation. However, given the toxicity of VirB1* to yeast, we do not intend that the data in Table 3 represent an exact quantitative assessment of these interactions. Nevertheless, the data are qualitatively sound and highly reproducible. Interestingly, we have shown previously that reduced expression of toxic proteins leads to higher levels of yeast two-hybrid interactions (as assessed by measuring the β-galactosidase activity) (25). Thus, protein levels per se cannot be used to monitor the strength of different protein-protein interactions.

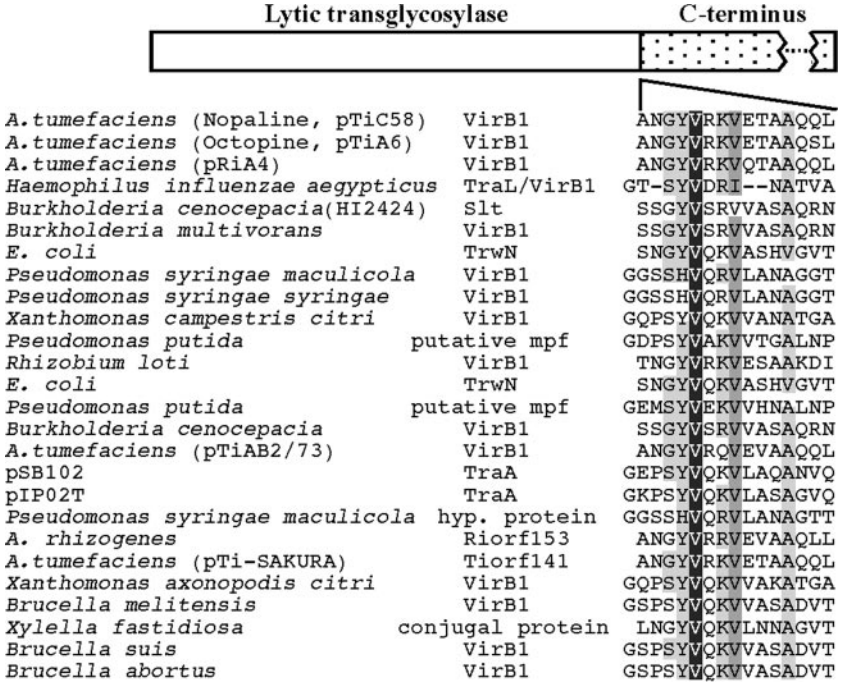

FIG. 8. Conservation of B1* processing site in homologs of nopaline VirB1. The schematic representation of VirB1 shows the region of N-terminal lytic transglycosylase homology and the divergent C terminus. Twenty-five nopaline VirB1 (pTiC58) homologs were identified with homology to the processing site of VirB1* (indicated at junction between the N and C termini) from *A. tumefaciens* (C58). Increasing conservation is indicated by darker shading.

A

VirB1 Construct	Mean number of YD116 colonies per μg plasmid DNA (std. dev.) (n=3 transformations)
VirB1	2945(445)
VirBΔSP	39(6)
VirB1*+44	1635(333)
VirB1*	15(0)

B

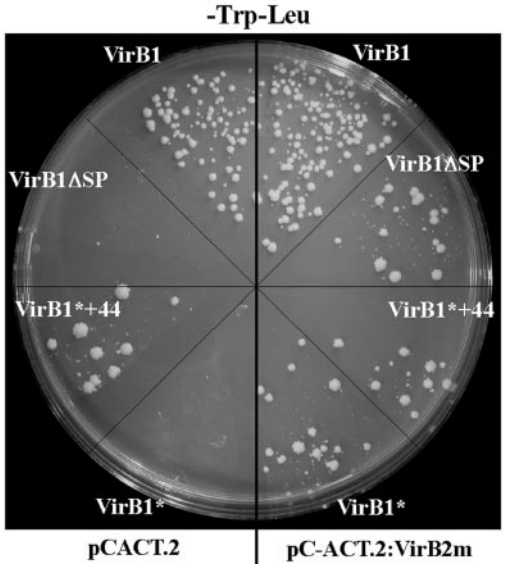

FIG. 9. Toxicity of VirB1* to yeast is mitigated by coexpression of VirB2m. Aliquots of yeast transformations were plated on medium to select for maintenance of both the DNA-binding domain and activation domain plasmids. (A) Cotransformations of yeast with VirB1ΔSP or VirB1* and the empty activation domain plasmid are significantly less efficient than cotransformations of wild-type VirB1 or VirB1*+44 and the empty activation domain plasmid. (B) VirB1* and VirB1ΔSP toxicity (left side of the plate) is reduced by cotransformation with VirB2m (right side of the petri plate).

DISCUSSION

Partial restoration of virulence to a *virB1* deletion strain of *A. tumefaciens* by expression of either the N-terminal two-thirds of VirB1, which includes the lytic transglycosylase domain (75), or the C-terminal VirB1* suggests that each domain makes a unique contribution to virulence (53, 54). Since proteins larger than 25 to 50 kDa cannot pass through naturally occurring channels in the intact peptidoglycan matrix (21), this matrix would prevent elaboration of the *vir*-T4SS, which contains subassemblies containing VirB8, VirB9, and VirB10 that are at least 230 kDa (47). Therefore, it is likely that modification of the peptidoglycan is a necessary prerequisite to the assembly of the *vir*-T4SS. The N-terminal lytic transglycosylase VirB1 interactions with periplasmic VirB8 and VirB10 suggest that transglycosylase activity of VirB1 is regulated by targeting it specifically to sites of *vir*-T4SS assembly (72), which would also prevent excessive degradation of the cell wall (5). Not all T4SS have a *virB1* homolog (e.g., *avhB* in *A. tumefaciens* [12]), and deletion of *virB1* homologs reduces but does not abolish function. Perhaps in these cases, other, non-T4SS transglycosylases are recruited to the site of assembly by one or more of the T4SS components, similar to the proposed localization of VirB1 via interactions with VirB8 and VirB10 (37, 72).

No role for the C terminus of VirB1, VirB1*, has been proposed previously. A database search with the amino acid sequence of VirB1* did not identify any related proteins other than VirB1 homologs primarily from strains of *A. tumefaciens* or closely related species (nine from *A. tumefaciens*, one from *A. rhizogenes*, one from *Rhizobium etli*, and one from *Mesorhizobium loti*; J. Zupan, O. Draper, R. Middleton, and P. Zambryski, data not shown). Therefore, no role for VirB1* can be inferred from proteins that function in systems or processes other than T4SS.

Evidence for processing a C-terminal product from VirB1 homologs is emerging. The machinery to process and secrete VirB1* from VirB1 (pTiC58, nopaline) is conserved in an octopine strain (A348) of *A. tumefaciens* (53). In addition, we now detect a protein of approximately 13 kDa with an anti-hemagglutinin antibody in cell lysates of *vir*-induced A348ΔB1 that expressed octopine VirB1 with hemagglutinin tags. VirB1* processing, or stability, in the octopine system was affected by the position of the epitope tag. Octopine VirB1* with an internal hemagglutinin tag was produced at an efficiency comparable to the nopaline system. In contrast, the hemagglutinin tag at the carboxy terminus of VirB1* severely reduced the amount of VirB1* produced. Both nopaline and octopine strains process and secrete a nopaline VirB1 variant [VirB(Q/S)], where the VirB1* processing site was altered to conform to the amino acid sequence of octopine VirB1 in this region. Recently, a VirB1*candidate has been identified in the cell lysate of *Brucella abortus* (20). Finally, homology searches identified a set of VirB1 homologs that exhibit sequence similarity in their C termini in addition to the region of lytic transglycosylase similarity. The carboxy-terminal homology among these latter proteins is confined to a region of about 10 aa at the VirB1* processing site; sequences distal to this domain diverge (see Fig. S1 in the supplemental material). Together, these data suggest that C-terminal processing of VirB1-like proteins may not be restricted to *A. tumefaciens*.

In the present study, the abundance of VirB2 and VirB5 in isolated T pili was positively correlated with the presence of VirB1* but not the lytic transglycosylase N-terminal domain of VirB1. VirB1* also is found in isolated T pili. In addition, VirB1* bound significantly to mature T-pilus subunits VirB2 (aa 48 to 121) and VirB5ΔSP in the yeast two-hybrid assay. Thus, genetic, cell fractionation, microscopy data from *A. tumefaciens* and physical interaction data from the yeast two-hybrid system together suggest that VirB1* facilitates T-pilus biogenesis by binding to VirB2 as well as to VirB5.

The interaction between VirB1* and the structural T-pilus components, VirB2 and VirB5, may contribute to the regulation of T-pilus biogenesis. Assembly of a polymeric, extracellular structure such as the T-pilus likely requires mechanisms that ensure temporal and spatial control of subunit interaction. Presumably, T-pilus assembly is at least partly driven by the interaction between regions on the surface of the VirB2 and VirB5 proteins. VirB1* may bind VirB2 and VirB5 monomers at the inner membrane or in the periplasm, thereby masking VirB2-VirB2 or VirB2-VirB5 interaction domains until they

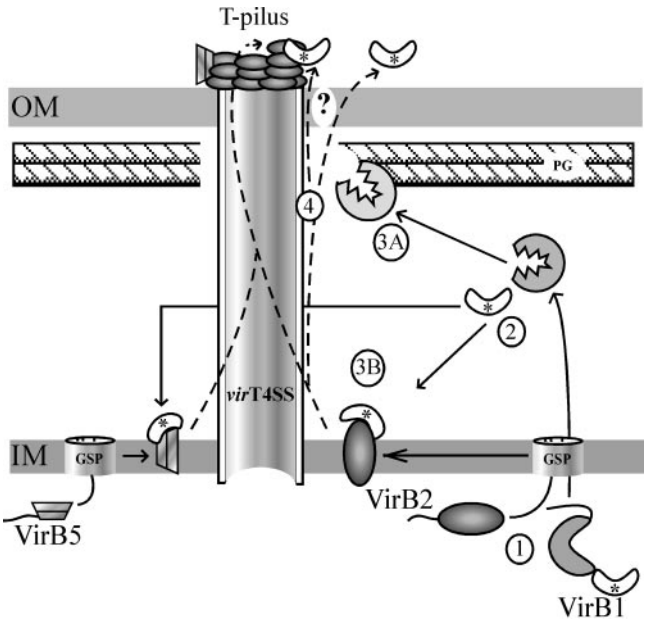

FIG. 10. Model depicting functions of VirB1 in assembly of the *vir*-T4SS. (Step 1) VirB1, VirB2, and VirB5 are translocated to the inner membrane via the GSP. Signal peptides (SPI) domains are represented by black wavy lines at the left N-terminal end of each protein. (Step 2) Signal peptides are now removed from VirB1, VirB2, and VirB5. VirB1 is processed to release VirB1* from lytic transglycosylase domain. (Step 3A) Lytic transglycosylase domain degrades peptidoglycan (PG) to create space for assembly of the *vir*-T4SS trans-envelope core. (Step 3B) VirB1* binds to VirB2 and VirB5 during their transit from the GSP to the cell exterior. (Step 4) At the site of T-pilus assembly,VirB2 and VirB5 are mobilized to the exterior of the cell. Mobilization of VirB1* to cell exterior does not require any additional Vir proteins (53). A fraction of VirB1* remains associated with T pili, while some VirB1* is free in the medium. VirB2 is drawn as a shaded oval to represent the cyclized form of the mature peptide. VirB5 is drawn as shaded stacked trapezoids to represent the helix bundles of the solved structure of VirB5 (73). The VirB5 trapezoid is shown localized at the base of the T pilus; however, its precise localization within the T-pilus structure remains to be determined. VirB1 is shown with two domain structures. The N terminus of VirB1 in the periplasm is shown as a "Pac-Man" due to the function of this lytic transglycosylase-homologous domain to "chew" the peptidoglycan. C-terminal VirB1* is drawn as a white ellipsoid. *, VirB1*; ?, unknown exporter for VirB1*; IM, inner membrane; OM, outer membrane.

are utilized at the site of T-pilus assembly. Since significant amounts of VirB1* are found on the cell exterior and associated with the T pilus, some VirB1* may remain associated with T-pilus subunits during their transit across the outer membrane.

Many type 2, type 3, and type 4 secretion systems mediate the biogenesis of cell surface-associated filamentous or fibrous structures that mediate adhesion to the host cell surface (67). In each case, there is a requirement for the spatiotemporal regulation of assembly of these structures (68). In some cases, regulation of assembly is mediated by periplasmic chaperones; the best known are members of the PapD-like superfamily (39). PapD-like proteins not only bind P-pilus subunits in the periplasm of pathogenic *E. coli* but also facilitate proper folding after the subunit emerges from the GSP into the periplasm in an unfolded state. Although VirB1* is proposed to bind T-pilus subunits and promote their accumulation in T pili, it is not known whether VirB1* performs all of the functions provided by PapD-like chaperones. Additional chaperone-like characteristics of VirB1* are its low molecular weight and acidic pI, which are common characteristics of type III secretion system chaperones (57). Alternatively, VirB1* binding may mediate some other step in T-pilus biogenesis, such as recruitment of VirB2 and VirB5 to the core transporter via interactions between VirB1 and VirB8, VirB9, or VirB10 (72).

We propose that VirB1 is a bifunctional protein for the biogenesis of the *vir*-T4SS (Fig. 10). The N-terminal lytic transglycosylase domain would provide localized modification of the peptidoglycan to create pores large enough for the assembly of the *vir*-T4SS trans-envelope core. The C-terminal VirB1* would regulate T-pilus assembly by binding T-pilus subunits, possibly to prevent their premature association. VirB1* on the cell exterior and in the T-pilus fraction may be cotransported with T-pilus subunits or may reflect residual binding of VirB1* to VirB2 or VirB5 after T-pilus assembly. Future studies will address the impact of *virB1* deletion on the assembly of the T4SS core, as well as the identity of the VirB1* protease. These studies likely have broad significance since many T4SS, as well as type III secretion systems, have VirB1 homologs (46), and their assembly requires both penetration of the peptidoglycan layer and mobilization of structural components to the exterior of the cell.

ACKNOWLEDGMENTS

We thank Christian Baron for the gift of anti-VirB2 antibody. We thank Peter Christie for the octopine strain A348ΔB1. We thank Kent McDonald, director of the University of California, Berkeley, Electron Microscope Laboratory, for assistance with transmission electron microscopy. We thank Rebecca Middleton for help with sequence analysis.

C.A.H. was supported by an NSF predoctoral fellowship. J.A. was supported by a UC Berkeley Chancellors Fellowship. This research was supported by a grant from the NSF (MCB-0343566) awarded to P.Z.

REFERENCES

1. **Atmakuri, K., E. Cascales, and P. J. Christie.** 2004. Energetic components VirD4, VirB11 and VirB4 mediate early DNA transfer reactions required for bacterial type IV secretion. Mol. Microbiol. **54:**1199–1211.
2. **Baron, C., N. Domke, M. Beinhofer, and S. Hapfelmeier.** 2001. Elevated temperature differentially affects virulence, VirB protein accumulation, and T-pilus formation in different *Agrobacterium tumefaciens* and *Agrobacterium vitis* strains. J. Bacteriol. **183:**6852–6861.
3. **Baron, C., M. Llosa, S. Zhou, and P. C. Zambryski.** 1997. VirB1, a component of the T-complex transfer machinery of *Agrobacterium tumefaciens*, is processed to a C-terminal secreted product, VirB1. J. Bacteriol. **179:**1203–1210.
4. **Baron, C., Y. R. Thorstenson, and P. C. Zambryski.** 1997. The lipoprotein VirB7 interacts with VirB9 in the membranes of *Agrobacterium tumefaciens*. J. Bacteriol. **179:**1211–1218.
5. **Bayer, M., K. Bischof, R. Noiges, and G. Koraimann.** 2000. Subcellular localization and processing of the lytic transglycosylase of the conjugative plasmid R1. FEBS Lett. **466:**389–393.
6. **Berger, B. R., and P. J. Christie.** 1994. Genetic complementation analysis of the *Agrobacterium tumefaciens virB* operon: *virB2* through *virB11* are essential virulence genes. J. Bacteriol. **176:**3646–3660.
7. **Blocker, A., K. Komoriya, and S. Aizawa.** 2003. Type III secretion systems and bacterial flagella: insights into their function from structural similarities. Proc. Natl. Acad. Sci. USA **100:**3027–3030.
8. **Bohne, J., A. Yim, and A. N. Binns.** 1998. The Ti plasmid increases the efficiency of *Agrobacterium tumefaciens* as a recipient in *virB*-mediated conjugal transfer of an IncQ plasmid. Proc. Natl. Acad. Sci. USA **95:**7057–7062.
9. **Cascales, E., and P. J. Christie.** 2004. *Agrobacterium* VirB10, an ATP energy sensor required for type IV secretion. Proc. Natl. Acad. Sci. USA:0405843101.
10. **Cascales, E., and P. J. Christie.** 2004. Definition of a bacterial type IV secretion pathway for a DNA substrate. Science **304:**1170–1173.
11. **Cascales, E., and P. J. Christie.** 2003. The versatile bacterial type IV secretion systems. Nat. Rev. Microbiol. **1:**137–149.

12. **Chen, L., Y. Chen, D. W. Wood, and E. W. Nester.** 2002. A new type IV secretion system promotes conjugal transfer in *Agrobacterium tumefaciens*. J. Bacteriol. **184:**4838–4845.
13. **Christie, P. J.** 1997. *Agrobacterium tumefaciens* T-complex transport apparatus: a paradigm for a new family of multifunctional transporters in eubacteria. J. Bacteriol. **179:**3085–3094.
14. **Christie, P. J.** 2004. Type IV secretion: the *Agrobacterium* VirB/D4 and related conjugation systems. Biochim. Biophys. Acta **1694:**219–234.
15. **Christie, P. J., K. Atmakuri, V. Krishnamoorthy, S. Jakubowski, and E. Cascales.** 2005. Biogenesis, architecture, and function of bacterial type IV secretion systems. Annu. Rev. Microbiol. **59:**451–485.
16. **Clamp, M., J. Cuff, S. M. Searle, and G. J. Barton.** 2004. The Jalview Java alignment editor. Bioinformatics **20:**426–427.
17. **Dang, T. A., and P. J. Christie.** 1997. The VirB4 ATPase of *Agrobacterium tumefaciens* is a cytoplasmic membrane protein exposed at the periplasmic surface. J. Bacteriol. **179:**453–462.
18. **Dang, T. A., X. R. Zhou, B. Graf, and P. J. Christie.** 1999. Dimerization of the *Agrobacterium tumefaciens* VirB4 ATPase and the effect of ATP-binding cassette mutations on the assembly and function of the T-DNA transporter. Mol. Microbiol. **32:**1239–1253.
19. **de Maagd, R. A., and B. Lugtenberg.** 1986. Fractionation of *Rhizobium leguminosarum* cells into outer membrane, cytoplasmic membrane, periplasmic, and cytoplasmic components. J. Bacteriol. **167:**1083–1085.
20. **den Hartigh, A. B., Y. H. Sun, D. Sondervan, N. Heuvelmans, M. O. Reinders, T. A. Ficht, and R. M. Tsolis.** 2004. Differential requirements for VirB1 and VirB2 during *Brucella abortus* infection. Infect. Immun. **72:**5143–5149.
21. **Dijkstra, A. J., and W. Keck.** 1996. Peptidoglycan as a barrier to transenvelope transport. J. Bacteriol. **178:**5555–5562.
22. **Ding, Z., K. Atmakuri, and P. J. Christie.** 2003. The outs and ins of bacterial type IV secretion substrates. Trends Microbiol. **11:**527–535.
23. **Draper, O., R. Middleton, M. Doucleff, and P. C. Zambryski.** 2006. Topology of the VirB4 C terminus in the *Agrobacterium tumefaciens* VirB/D4 type IV secretion system. J. Biol. Chem. **281:**37628–37635.
24. **Durfee, T., K. Becherer, P. L. Chen, S. H. Yeh, Y. Yang, A. E. Kilburn, W. H. Lee, and S. J. Elledge.** 1993. The retinoblastoma protein associates with the protein phosphatase type 1 catalytic subunit. Genes Dev. **7:**555–569.
25. **Durfee, T., O. Draper, J. Zupan, D. S. Conklin, and P. C. Zambryski.** 1999. New tools for protein linkage mapping and general two-hybrid screening. Yeast **15:**1761–1768.
26. **Eddy, S. R.** 1998. Profile hidden Markov models. Bioinformatics **14:**755–763.
27. **Edgar, R. C.** 2004. MUSCLE: multiple sequence alignment with high accuracy and high throughput. Nucleic Acids Res. **32:**1792–1797.
28. **Eisenbrandt, R., M. Kalkum, E. M. Lai, R. Lurz, C. I. Kado, and E. Lanka.** 1999. Conjugative pili of IncP plasmids, and the Ti plasmid T pilus are composed of cyclic subunits. J. Biol. Chem. **274:**22548–22555.
29. **Fullner, K. J.** 1998. Role of *Agrobacterium virB* genes in transfer of T complexes and RSF1010. J. Bacteriol. **180:**430–434.
30. **Fullner, K. J., J. C. Lara, and E. W. Nester.** 1996. Pilus assembly by *Agrobacterium* T-DNA transfer genes. Science **273:**1107–1109.
31. **Fullner, K. J., K. M. Stephens, and E. W. Nester.** 1994. An essential virulence protein of *Agrobacterium tumefaciens*, VirB4, requires an intact mononucleotide binding domain to function in transfer of T-DNA. Mol. Gen. Genet. **245:**704–715.
32. **Gelvin, S. B.** 2003. Agrobacterium-mediated plant transformation: the biology behind the "gene-jockeying" tool. Microbiol. Mol. Biol. Rev. **67**:16–37.
33. **Gomis-Ruth, F. X., M. Sola, F. de la Cruz, and M. Coll.** 2004. Coupling factors in macromolecular type-IV secretion machineries. Curr. Pharm. Des. **10:**1551–1565.
34. **Goodner, B., G. Hinkle, S. Gattung, N. Miller, M. Blanchard, B. Qurollo, B. S. Goldman, Y. Cao, M. Askenazi, C. Halling, L. Mullin, K. Houmiel, J. Gordon, M. Vaudin, O. Iartchouk, A. Epp, F. Liu, C. Wollam, M. Allinger, D. Doughty, C. Scott, C. Lappas, B. Markelz, C. Flanagan, C. Crowell, J. Gurson, C. Lomo, C. Sear, G. Strub, C. Cielo, and S. Slater.** 2001. Genome sequence of the plant pathogen and biotechnology agent *Agrobacterium tumefaciens* C58. Science **294:**2323–2328.
35. **Grohmann, E., G. Muth, and M. Espinosa.** 2003. Conjugative plasmid transfer in gram-positive bacteria. Microbiol. Mol. Biol. Rev. **67:**277–301.
36. **Hapfelmeier, S., N. Domke, P. C. Zambryski, and C. Baron.** 2000. VirB6 is required for stabilization of VirB5 and VirB3 and formation of VirB7 homodimers in *Agrobacterium tumefaciens*. J. Bacteriol. **182:**4505–4511.
37. **Hoppner, C., A. Carle, D. Sivanesan, S. Hoeppner, and C. Baron.** 2005. The putative lytic transglycosylase VirB1 from *Brucella suis* interacts with the type IV secretion system core components VirB8, VirB9, and VirB11. Microbiology **151:**3469–3482.
38. **Hoppner, C., Z. Liu, N. Domke, A. N. Binns, and C. Baron.** 2004. VirB1 orthologs from *Brucella suis* and pKM101 complement defects of the lytic transglycosylase required for efficient type IV secretion from *Agrobacterium tumefaciens*. J. Bacteriol. **186:**1415–1422.
39. **Hultgren, S. J., S. Abraham, M. Caparon, P. Falk, J. W. D. St. Geme, and S. Normark.** 1993. Pilus and nonpilus bacterial adhesins: assembly and function in cell recognition. Cell **73**:887–901.
40. **Itoh, Y., J. M. Watson, D. Haas, and T. Leisinger.** 1984. Genetic and molecular characterization of the *Pseudomonas* plasmid pVS1. Plasmid **11:**206–220.
41. **Jakubowski, S. J., E. Cascales, V. Krishnamoorthy, and P. J. Christie.** 2005. *Agrobacterium tumefaciens* VirB9, an outer-membrane-associated component of a type IV secretion system, regulates substrate selection and T-pilus biogenesis. J. Bacteriol. **187:**3486–3495.
42. **Jakubowski, S. J., V. Krishnamoorthy, and P. J. Christie.** 2003. *Agrobacterium tumefaciens* VirB6 protein participates in formation of VirB7 and VirB9 complexes required for type IV secretion. J. Bacteriol. **185:**2867–2878.
43. **Judd, P. K., R. B. Kumar, and A. Das.** 2005. Spatial location and requirements for the assembly of the *Agrobacterium tumefaciens* type IV secretion apparatus. Proc. Natl. Acad. Sci. USA **102:**11498–11503.
44. **Judd, P. K., D. Mahli, and A. Das.** 2005. Molecular characterization of the *Agrobacterium tumefaciens* DNA transfer protein VirB6. Microbiology **151:**3483–3492.
45. **Koonin, E. V., and K. E. Rudd.** 1994. A conserved domain in putative bacterial and bacteriophage transglycosylases. Trends Biochem. Sci. **19:**106–107.
46. **Koraimann, G.** 2003. Lytic transglycosylases in macromolecular transport systems of gram-negative bacteria. Cell Mol. Life Sci. **60:**2371–2388.
47. **Krall, L., U. Wiedemann, G. Unsin, S. Weiss, N. Domke, and C. Baron.** 2002. Detergent extraction identifies different VirB protein subassemblies of the type IV secretion machinery in the membranes of *Agrobacterium tumefaciens*. Proc. Natl. Acad. Sci. USA **99:**11405–11410.
48. **Kuldau, G. A., G. De Vos, J. Owen, G. McCaffrey, and P. Zambryski.** 1990. The *virB* operon of *Agrobacterium tumefaciens* pTiC58 encodes 11 open reading frames. Mol. Gen. Genet. **221:**256–266.
49. **Lai, E. M., O. Chesnokova, L. M. Banta, and C. I. Kado.** 2000. Genetic and environmental factors affecting T-pilin export and T-pilus biogenesis in relation to flagellation of *Agrobacterium tumefaciens*. J. Bacteriol. **182:**3705–3716.
50. **Lai, E. M., and C. I. Kado.** 1998. Processed VirB2 is the major subunit of the promiscuous pilus of *Agrobacterium tumefaciens*. J. Bacteriol. **180:**2711–2717.
51. **Lai, E. M., and C. I. Kado.** 2000. The T-pilus of *Agrobacterium tumefaciens*. Trends Microbiol. **8:**361–369.
52. **Llosa, M., and D. O'Callaghan.** 2004. Euroconference on the Biology of Type IV Secretion Processes: Bacterial Gates into the Outer World. Mol. Microbiol. **53**:1–8.
53. **Llosa, M., J. Zupan, C. Baron, and P. Zambryski.** 2000. The N- and C-terminal portions of the *Agrobacterium* VirB1 protein independently enhance tumorigenesis. J. Bacteriol. **182:**3437–3445.
54. **Mushegian, A. R., K. J. Fullner, E. V. Koonin, and E. W. Nester.** 1996. A family of lysozyme-like virulence factors in bacterial pathogens of plants and animals. Proc. Natl. Acad. Sci. USA **93:**7321–7326.
55. **Nagai, H., and C. R. Roy.** 2003. Show me the substrates: modulation of host cell function by type IV secretion systems. Cell Microbiol. **5:**373–383.
56. **Ochman, H., A. S. Gerber, and D. L. Hartl.** 1988. Genetic applications of an inverse polymerase chain reaction. Genetics **120:**621–623.
57. **Parsot, C., C. Hamiaux, and A. L. Page.** 2003. The various and varying roles of specific chaperones in type III secretion systems. Curr. Opin. Microbiol. **6:**7–14.
58. **Peabody, C. R., Y. J. Chung, M. R. Yen, D. Vidal-Ingigliardi, A. P. Pugsley, and M. H. Saier, Jr.** 2003. Type II protein secretion and its relationship to bacterial type IV pili and archaeal flagella. Microbiology **149**:3051–3072.
59. **Remaut, H., and G. Waksman.** 2004. Structural biology of bacterial pathogenesis. Curr. Opin. Struct. Biol. **14:**161–170.
60. **Sagulenko, V., E. Sagulenko, S. Jakubowski, E. Spudich, and P. J. Christie.** 2001. VirB7 lipoprotein is exocellular and associates with the *Agrobacterium tumefaciens* T pilus. J. Bacteriol. **183:**3642–3651.
61. **Sambrook, J., E. F. Fritsch, and T. Maniatis.** 1989. Molecular cloning: a laboratory manual, 2nd ed. Cold Spring Harbor Laboratory Press, Cold Spring Harbor, NY.
62. **Schmidt-Eisenlohr, H., N. Domke, C. Angerer, G. Wanner, P. C. Zambryski, and C. Baron.** 1999. Vir proteins stabilize VirB5 and mediate its association with the T pilus of *Agrobacterium tumefaciens*. J. Bacteriol. **181:**7485–7492.
63. **Schmidt-Eisenlohr, H., N. Domke, and C. Baron.** TraC of IncN plasmid pKM101 associates with membranes and extracellular high molecular weight structures in *Escherichia coli*. J. Bacteriol., in press.
64. **Schrammeijer, B., A. den Dulk-Ras, A. C. Vergunst, E. Jurado Jacome, and P. J. Hooykaas.** 2003. Analysis of Vir protein translocation from *Agrobacterium tumefaciens* using *Saccharomyces cerevisiae* as a model: evidence for transport of a novel effector protein VirE3. Nucleic Acids Res. **31:**860–868.
65. **Shirasu, K., Z. Koukolikova-Nicola, B. Hohn, and C. I. Kado.** 1994. An inner-membrane-associated virulence protein essential for T-DNA transfer from *Agrobacterium tumefaciens* to plants exhibits ATPase activity and similarities to conjugative transfer genes. Mol. Microbiol. **11:**581–588.
66. **Simone, M., C. A. McCullen, L. E. Stahl, and A. N. Binns.** 2001. The carboxy terminus of VirE2 from *Agrobacterium tumefaciens* is required for its transport to host cells by the *virB*-encoded type IV transport system. Mol. Microbiol. **41:**1283–1293.
67. **Thanassi, D. G., and S. J. Hultgren.** 2000. Multiple pathways allow protein

secretion across the bacterial outer membrane. Curr. Opin. Cell Biol. **12:** 420–430.

68. **Thanassi, D. G., E. T. Saulino, and S. J. Hultgren.** 1998. The chaperone/usher pathway: a major terminal branch of the general secretory pathway. Curr. Opin. Microbiol. **1:**223–231.
69. **Thorstenson, Y. R., G. A. Kuldau, and P. C. Zambryski.** 1993. Subcellular localization of seven VirB proteins of *Agrobacterium tumefaciens*: implications for the formation of a T-DNA transport structure. J. Bacteriol. **175:** 5233–5241.
70. **Vergunst, A. C., B. Schrammeijer, A. den Dulk-Ras, C. M. de Vlaam, T. J. Regensburg-Tuink, and P. J. Hooykaas.** 2000. VirB/D4-dependent protein translocation from *Agrobacterium* into plant cells. Science **290:**979–982.
71. **Vergunst, A. C., M. C. van Lier, A. den Dulk-Ras, T. A. Stuve, A. Ouwehand, and P. J. Hooykaas.** 2005. Positive charge is an important feature of the C-terminal transport signal of the VirB/D4-translocated proteins of *Agrobacterium*. Proc. Natl. Acad. Sci. USA **102:**832–837.
72. **Ward, D. V., O. Draper, J. R. Zupan, and P. C. Zambryski.** 2002. Peptide linkage mapping of the *Agrobacterium tumefaciens vir*-encoded type IV secretion system reveals protein subassemblies. Proc. Natl. Acad. Sci. USA **99:**11493–11500.
73. **Yeo, H. J., Q. Yuan, M. R. Beck, C. Baron, and G. Waksman.** 2003. Structural and functional characterization of the VirB5 protein from the type IV secretion system encoded by the conjugative plasmid pKM101. Proc. Natl. Acad. Sci. USA **100:**15947–15952.
74. **Yuan, Q., A. Carle, C. Gao, D. Sivanesan, K. A. Aly, C. Hoppner, L. Krall, N. Domke, and C. Baron.** 2005. Identification of the VirB4-VirB8-VirB5-VirB2 pilus assembly sequence of type IV secretion systems. J. Biol. Chem.
75. **Zahrl, D., M. Wagner, K. Bischof, M. Bayer, B. Zavecz, A. Beranek, C. Ruckenstuhl, G. E. Zarfel, and G. Koraimann.** 2005. Peptidoglycan degradation by specialized lytic transglycosylases associated with type III and type IV secretion systems. Microbiology **151:**3455–3467.
76. **Zhu, J., P. M. Oger, B. Schrammeijer, P. J. Hooykaas, S. K. Farrand, and S. C. Winans.** 2000. The bases of crown gall tumorigenesis. J. Bacteriol. **182:**3885–3895.
77. **Zupan, J., T. R. Muth, O. Draper, and P. Zambryski.** 2000. The transfer of DNA from *Agrobacterium tumefaciens* into plants: a feast of fundamental insights. Plant J. **23:**11–28.